Plasmon resonance shifts in oxide-coated silver nanoparticles

K. Chatterjee,[1] S. Banerjee,[2] and D. Chakravorty[1]
[1]*Indian Association for the Cultivation of Science, Jadavpur, Kolkata–700 032, India*
[2]*Department of Physics, Calcutta University, Kolkata–700 009, India*
(Received 4 February 2002; revised manuscript received 30 April 2002; published 30 August 2002)

Silver-silica nanocomposites have been synthesized by an electrodeposition technique. Silver oxide layers have been grown on the silver particles by an oxidation treatment of the nanocomposites in the temperature range 478–653 K. Optical absorption spectra of films of these nanocomposites dispersed in polystyrene were studied in the wavelength range 250–800 nm. Two absorption peaks were observed. The one around 370 nm is shown to be due to the uncoated silver nanoparticles. The other in the range 550–700 nm arises due to the presence of silver-core–silver-oxide nanoshells in these materials. The data were analyzed by the relevant theory of optical scattering from ultrafine composite particles which took into account the size-dependent dielectric permittivity of silver metal cores. The analysis indicates that nanoshells of thicknesses in the range 1.0–10.6 nm are grown on the metal core depending on the oxidation temperature. The metal cores having diameters equal to or less than 3 nm show an electrical conductivity which is less than Mott's minimum metallic conductivity. The analysis of the first absorption peak also leads to the conclusion that the silver metal particles causing this absorption show a metal-insulator Mott transition. This implies that the metal particles have diameters less than 3 nm. The growth rate of the nanoshell indicates an activation energy of 0.29 eV, which is consistent with that for oxygen diffusion in a silicate glass.

DOI: 10.1103/PhysRevB.66.085421 PACS number(s): 78.66.Jg, 81.07.−b, 78.20.Ci, 36.40.Gk

INTRODUCTION

The optical properties of metal nanoparticles embedded in a dielectric medium have been a subject of immense interest in recent years because of their novel characteristics and possible device applications.[1–10] Different synthetic techniques have been used by different authors to prepare such nanocomposites. The absorption characteristics have been analyzed by Mie scattering theory[11] or the effective medium approach.[12] In most of these investigations nanoparticle plasmon resonance has been shown to be the major cause for the change in optical absorption behavior as a function of the metal particle size. An interesting system which has been lately studied extensively is heterostructure nanoparticles.[4,10] Enormous shifts of the optical absorption peak have been reported in the case of gold-coated nanoparticles of gold-sulfide (Au_2S) during the formation of the gold nanoshells around the dielectric core during the reduction process of Au_2S.[4] This was attributed to quantum confinement of carriers in the gold-shell layer. A more detailed analysis of the absorption behavior in this system, however, shows that the peak shift is purely classical in origin and is determined by the relative thickness of the gold shell and Au_2S core diameter.[10] We have recently been looking at the electrical properties emanating from a metal-core–metal-oxide shell nanostructure grown in a percolative configuration within a silica gel. The electrical conductivity shows several orders of magnitude increase as compared to that of the precursor gel.[13] The effect has been adduced to the presence of a amorphous phase at the interfaces of the oxide nanoshells. Our studies have so far been carried out on copper-copper oxide[13] and iron-iron oxide systems respectively.[14] As part of this wider investigation, we have prepared a silver-silver oxide core-shell nanostructure in a silica gel and studied the optical absorption. An analysis of the results lead to an interesting conclusion, viz., the nanosized silver particles having diameters equal to or less than ~3 nm have electrical conductivities less than Mott's minimum metallic conductivity. The details are reported in this paper.

EXPERIMENT

Nanocomposites containing silver particles in a silica matrix were prepared by an electrodeposition method the principles of which were elucidated earlier.[15,16] In the present work a gel was synthesized with a target composition 20 $AgNO_3$ and 80 SiO_2 (in mole percent). The precursor chemicals used were silver nitrate, tetraethylorthosilicate, and ethyl alcohol, respectively. A weighed amount of $AgNO_3$ was dissolved in water and ethyl alcohol and the mixture stirred in a magnetic stirrer vigorously for $\frac{1}{2}$ h to ensure complete dissolution of the salt. A measured volume of tetraethylorthosilicate was poured into the above solution, and one drop of 11 N nitric acid was added in order to maintain the *p*H of the final solution to a value of 5. Stirring was continued for 3 h, and a clear sol was obtained. The latter was poured into a flat bottomed plastic Petri dish and kept in darkness under ordinary atmosphere for 2 weeks for gelation. Transparent gel was obtained in the process. Gel pieces of typical dimensions 5 mm×5 mm×0.5 mm were taken and crushed in a mortar to an average size of ~5 μm. Silver nanoparticles were grown within the gel by an electrodeposition process.[15] A thick paste was first of all prepared by mixing 10 mg of the gel powder with 0.2 cm^3 of distilled water. An optically polished silver cathode of dimensions 4 cm×4 cm×0.1 mm was used here. An area of ~5 cm^2 of the cathode was painted with the paste prepared as above. The latter was dried by passing hot air above it at a temperature of 333 K for a few minutes. A polished silver plate anode of size 4 cm×1 cm ×0.5 mm was placed on the paste. A voltage of 20 V was

applied across the cell at room temperature. The current flowing through the circuit increased from a few microamperes to a few hundred milliamperes within 10 sec. This indicated that silver metal channels had formed within the gel. By shifting the anode plate to different positions and repeating the electrodeposition process, metal formation was achieved over the entire area of the paste. The cathode plate with the metallized paste was dried in an oven at a temperature of 353 K for 6 h. As reported earlier, the metallic chains formed consist of nanoparticles of silver connected to each other.[16] The gel powder with silver metal phase present within was scraped off the cathode plate with a blunt tweezer. The gel powder containing silver particles was subjected to heat treatment at ordinary atmosphere at temperatures ranging from 478 to 653 K for a duration of $\frac{1}{2}$ h. This was done to grow oxide layers on the metal particles.

For preparing a nanocomposite film 1 mg of gel powder prepared as above was taken in a test tube and 1 cm^3 of tetrahydrofuran (THF) was added to it. The mixture was kept in an ultrasonic bath for 10 min. Another solution was prepared by dissolving 0.2 g polystyrene in 20 cm^3 of THF. The two solutions were thoroughly mixed. A Corning 7059 glass slide of dimensions 3 cm$\times$1 cm$\times$0.1 cm after being cleaned in acetone was dipped into the above solution and drawn at a speed of $\sim$5 mm/sec. The typical thickness of films prepared and as measured by an optical microscope was $\sim$4 μm.

Optical absorption spectra of different nanocomposite films were recorded at room temperature in a UV-2101 PC UV-VIS scanning spectrophotometer manufactured by Shimadzu, Japan. Before taking the spectrum, the base line was corrected by placing two reference polystyrene films prepared by a method similar to that described above and having equal thickness at two beam positions. Optical absorption was measured for various samples, keeping one reference glass slide at the reference beam position. The absorption coefficient α at any wavelength was calculated from the relation

$$\alpha = \frac{2.3 d_o}{t}, \tag{1}$$

where $\mathbf{d}_o$ is the optical density of the sample and t is the film thickness.

The microstructure of different gel powders containing oxide-coated silver particles was studied by a JEM 200 CX transmission electron microscope. The method of sample preparation has been discussed earlier.[17]

RESULTS AND DISCUSSION

Figure 1(a) shows the electron micrograph for the specimen which was given an oxidation treatment at 478 K. Figure 1(b) is the electron diffraction pattern obtained from Fig. 1(a). The values of interplanar spacings $\mathbf{d}_{hkl}$ were calculated from the diameters of the diffraction rings. These are summarized in Table I. The experimentally, deduced $\mathbf{d}_{hkl}$ values are also compared in this table with the standard ASTM data for silver and silver oxide phases, respectively. It is evident from this table that both silver and silver oxide phases are present in the nanocomposite specimen. Such an observation

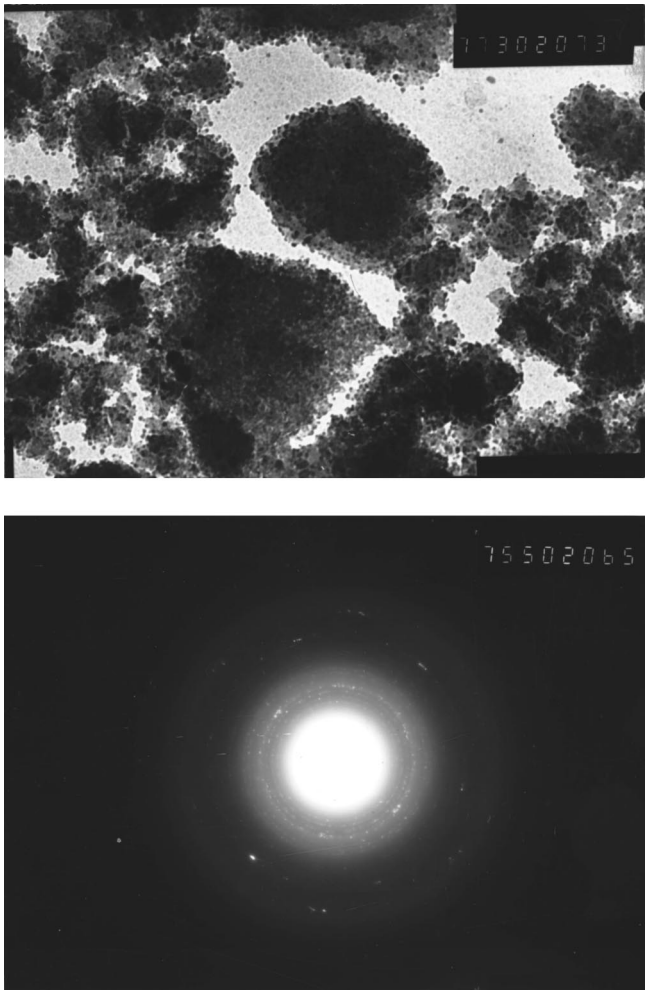

FIG. 1. Transmission electron micrograph for the nanocomposite specimen subjected to oxidation treatment at 478 K for $\frac{1}{2}$ h. (b) Electron diffraction pattern of (a).

is typical for other specimens also. We have recorded only one diffraction ring for the case of the present sample which could equally well be due to the Ag_2O phase. It is to be noted though that the diffraction ring obtained corresponds to the most intense line (d_{hkl}=0.2359 nm) from metallic silver as given in standard x-ray data. Similarly, the most intense diffraction line in the case of Ag_2O corresponds to d_{hkl}

TABLE I. Comparison of d_{hkl} values obtained from electron diffraction with standard ASTM data for specimens subjected to electrodeposition at 20 V followed by oxidation treatment at 478 K.

Observed d_{hkl} (nm)	Standard ASTM data	
	Silver (nm)	Silver oxide (nm)
0.27		0.2734
0.35		0.3348
0.23	0.2359	0.2367
0.16		0.1674
0.14		0.1427

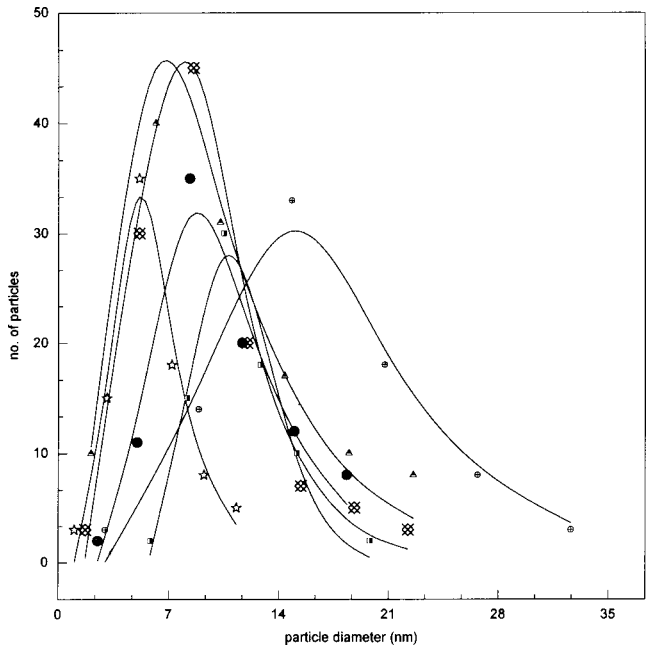

FIG. 2. Histogram of particle sizes as obtained from the transmission electron microscopy (TEM) of different specimens: (☆) Oxidation at 478 K/$\frac{1}{2}$ h, $\bar{x}=5.6$ nm, $\eta=1.5$; (⊗) 513 K/$\frac{1}{2}$ h, $\bar{x}=9.0$ nm, $\eta=1.5$; (◨) 548 K/$\frac{1}{2}$ h, $\bar{x}=11.2$ nm, $\eta=1.2$; (⊕) 583 K/$\frac{1}{2}$ h, $\bar{x}=16.6$ nm, $\eta=1.5$; (◑) 613 K/$\frac{1}{2}$ h, $\bar{x}=10.6$ nm, $\eta=1.5$; (▲) 653 K/$\frac{1}{2}$ h, $\bar{x}=9.1$ nm, $\eta=1.7$.

$=0.2734$ nm. Hence our conclusion regarding the presence of both Ag and Ag_2O in the nanocomposites is justified. Also, as we show subsequently that the optical absorption maximum observed around 370 nm provides a strong confirmation of the fact that silver metal particles are indeed present. It was reported earlier[18] that a silicate glass containing silver nanoparticles of diameter ~10 nm has an optical absorption maximum at ~400 nm. These data also show that silica glass does not exhibit any absorption peak in the wavelength range under consideration. It has also been reported[19] that Ag_2O particles do not show any absorption peak in the 370–400 nm range. In Fig. 2 we show the histogram of the particle sizes as obtained from Fig. 1(a). We also show the histograms for other samples with the respective heat treatment conditions mentioned in the figure caption. The points represent the data obtained from the electron micrographs of different samples. The solid lines correspond to the curves fitted theoretically to the log-normal distribution function[20] given by

$$\Delta n=\left(\frac{1}{\sqrt{2\pi}\ln\eta}\right)\exp\left\{-\frac{1}{2}\left[\ln\left(\frac{x}{\bar{x}}\right)\Big/\ln\eta\right]^2\right\}\Delta(\ln x), \tag{2}$$

where Δn is the fractional number of particles, x is the diameter of the particle, $\bar{x}$ is the median diameter, and η is the geometric standard deviation. The extracted values of $\bar{x}$ and η for different specimens are shown in the figure caption. It is evident from these numbers that the median diameter of the composite particle increases up to a treatment temperature of 583 K. Beyond this temperature, however, the measured diameter shows a decreasing trend. This apparent anomaly arises due to the fact that Ag_2O is thermodynamically unstable at temperatures above 500 K when it dissociates into Ag and O_2.[21] Thus the two reactions—viz., oxidation of silver and dissociation of silver oxide to silver—proceed simultaneously. Above 583 K the latter reaction rate becomes larger than that of the former, and as a consequence we obtain smaller composite particles within the gel medium.

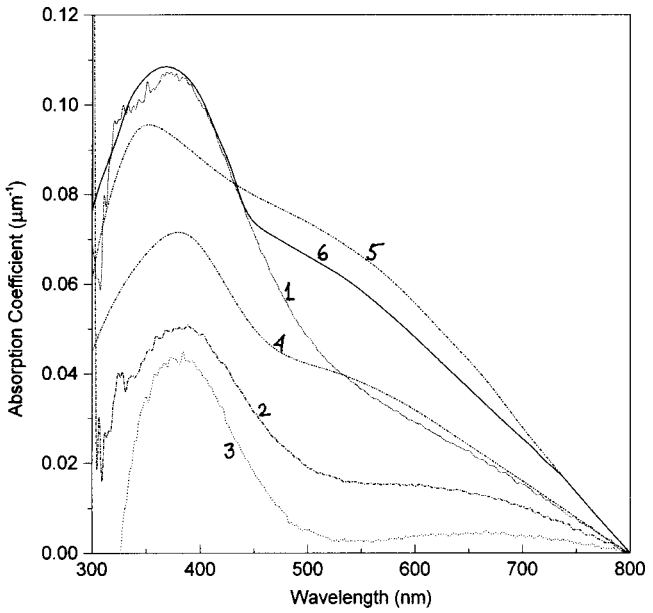

FIG. 3. Variation of optical absorption coefficient as a function of wavelength for different specimens Nos. 1–6.

Figure 3 shows the variation of absorption coefficient as a function of wavelength for different specimens. It is seen that there are two absorption peaks for all specimens: one around 370 nm and the other varying over the range 550–700 nm. We have analyzed these data on the basis of theories on optical properties of metal clusters as discussed below. The first peak which remains at ~370 nm for all the specimens with different oxidation treatments is shown to arise due to the plasmon resonance of silver nanoparticles. The second peak is due to the Ag_2O-coated Ag nanoparticles.

The Maxwell-Garnet model[22] is applicable in the case of a homogeneous medium in which equal-sized metal particles separated from each other are dispersed. The particles are assumed to scatter light independently. According to this model, the effective permittivity of the medium $\bar{\varepsilon}$ is given by

$$\bar{\varepsilon}=\frac{2f\varepsilon_m\varepsilon_h-2f\varepsilon_h^2+\varepsilon_m\varepsilon_h+2\varepsilon_h^2}{\varepsilon_m+2\varepsilon_h-f\varepsilon_m+f\varepsilon_h}, \tag{3}$$

where f is the volume fraction of the metal phase, ε_m is the dielectric permittivity of the metal phase, and ε_h is the dielectric permittivity of the silica gel phase. The absorption coefficient μ can be written as[23]

$$\mu=\frac{\omega}{c}\frac{\bar{\varepsilon}_2}{\sqrt{\varepsilon_1}}, \tag{4}$$

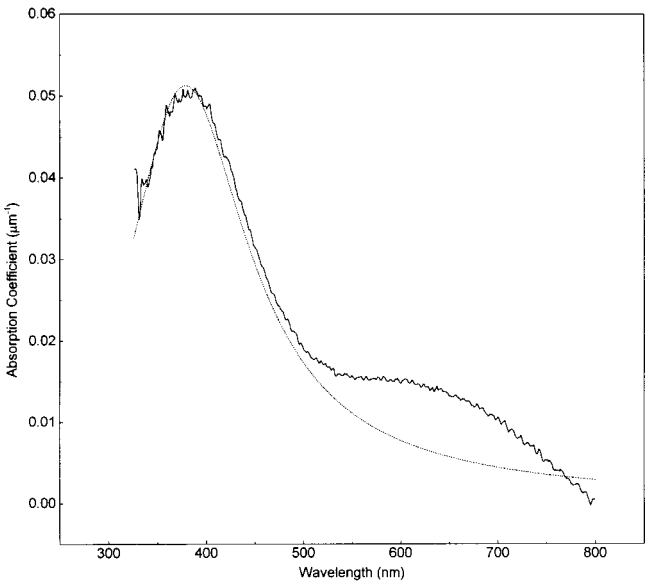

FIG. 4. Theoretical fit of the first peak for specimen No. 2 by the Maxwell-Garnett model: experimental (solid line) and theoretical (dotted line).

where ω is the angular frequency, c the velocity of light, and ε_1 and ε_2 are the real and imaginary parts of ε. We have fitted the first peak for all the specimens to Eqs. (3) and (4). The dielectric permittivity for the metal phase can be written as[24]

$$\varepsilon_m = 1 - \frac{\omega_p^2}{\omega^2 - i\omega\sigma/\varepsilon_0}, \tag{5}$$

where ω_p is the plasmon frequency for silver, σ is the conductivity of the silver particle, and ε_0 is the free-space permittivity.

We have calculated the bulk plasmon frequency for silver as 1.4×10^{16} rad/sec.[25] In order to fit the experimental data to the above theoretical model, we have taken σ, f, and ε_h as variables. In Fig. 4 we show the theoretical fit to experimental data for the first peak in optical absorption for specimen No. 2. This is typical for the other specimens also. Table II summarizes the values of the extracted parameters σ, f, and ε_h obtained by this curve fitting in the case of different specimens. It is seen that the volume fraction f is of the order of 10^{-4}. This justifies the application of the Maxwell-Garnett model to the present specimen system. The values of $\varepsilon_h = 3.8$ determined for all specimens is consistent with the fact that the matrix medium consists essentially of a silica glass. The values of σ found for all the specimens are below Mott's minimum metallic conductivity ($2.9\times10^4\ \Omega^{-1}\,\mathrm{m}^{-1}$) as calculated from the equation[26]

TABLE II. Extracted parameters σ, f, and ε_h obtained by a theoretical fitting to the Marwell-Garnett model for the first peak around 370 nm for different specimens.

Specimen No.	Oxidation treatment (K/$\frac{1}{2}$ h)	$\Omega\ \sigma$ (m^{-1})	f	ε_h
1	478	2.2×10^4	4.1×10^{-4}	3.8
2	513	1.8×10^4	1.6×10^{-4}	3.8
3	548	1.1×10^4	0.9×10^{-4}	3.8
4	583	2.2×10^4	2.9×10^{-4}	3.8
5	613	2.6×10^4	4.8×10^{-4}	3.8
6	653	2.5×10^4	4.9×10^{-4}	3.8

$$\sigma_{\min} = \left(\frac{e^2}{3\hbar\pi^2}\right) k_f, \tag{6}$$

where e is the electronic charge, h Planck's constant, and k_f the Fermi wave vector. It appears therefore that silver undergoes a metal-to-insulator transition when the particle size is below a particular value. The electron microscopic investigation gave us the size distribution for the composite metal-metal oxide particles. We will discuss the implication of the above result after discussing in the subsequent paragraphs the absorption behavior in the wavelength range 550–700 nm.

There is a distribution of particle sizes in our system, and each particle consists of a silver metal core with a shell comprising silver oxide. We therefore take into account the contribution from the various particle diameters with their shell thicknesses. The average polarizability for a silver particle with a silver oxide coating on it and embedded in a matrix is given by[4]

$$\alpha = \sum_j \frac{n_j r_j^3}{\Sigma n_j r_j^3} \left\{ \frac{(\varepsilon_s - \varepsilon_h)(\varepsilon_{mj} + 2\varepsilon_s) + \left(1 - \frac{t_j}{r_j}\right)^3 (\varepsilon_{mj} - \varepsilon_s)(\varepsilon_h + 2\varepsilon_s)}{(\varepsilon_{mj} + 2\varepsilon_s)(2\varepsilon_h + \varepsilon_s) + 2\left(1 - \frac{t_j}{r_j}\right)(\varepsilon_s - \varepsilon_h)(\varepsilon_{mj} - \varepsilon_s)} \right\} r_j^3, \tag{7}$$

where ε_s, ε_h, and ε_m are the dielectric permittivities of the shell, host medium, and metal core, respectively, n_j is the number of particles having radius r_j, and t_j is the thickness of the shell on the particle r_j. The size-dependent dielectric permittivity ε_{mj} in the case of a metal core for which the composite radius (i.e., inclusive of the shell) is r_j can be written as[24]

$$\varepsilon_{mj} = \left(1 - \frac{\omega_p^2}{\omega^2}\right) + i\left[\frac{\omega_p^2}{\omega^3}\left(\frac{\sigma_{mj}}{\varepsilon_o} + \frac{V_F}{r_j - t_j}\right)\right], \tag{8}$$

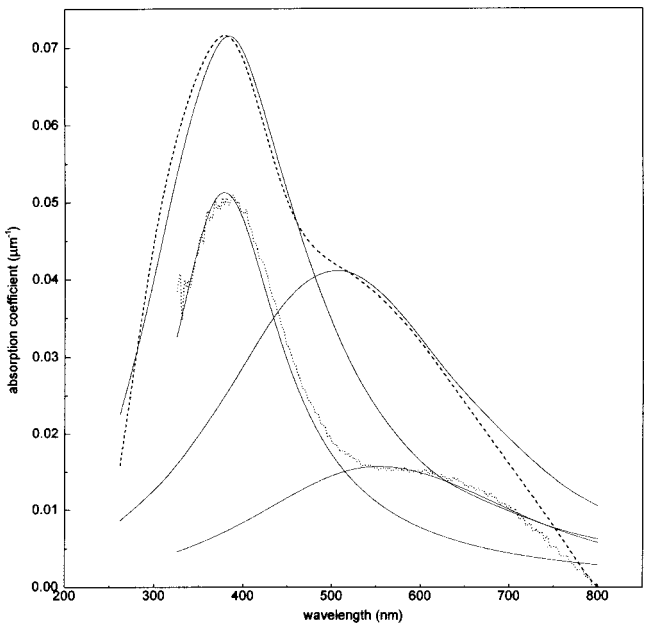

FIG. 5. Theoretical fit of experimental data: experimental specimen No. 2 (dotted line) and No. 4 (dashed line) and theory (solid line).

where ω_p is the bulk plasmon frequency, σ_{mj} is the conductivity of the metal core with radius $(r_j - t_j)$, ε_o is the free-space permittivity, and V_F is the Fermi velocity for silver. The dielectric permittivity for the composite system comprising the core-shell nanostructure within a gel medium can then be calculated using the Clausius-Mosotti relation as[25]

$$\varepsilon = \frac{1+2N\alpha}{1-N\alpha}, \tag{9}$$

where N is the number of particles per unit volume. The optical absorption coefficient μ can be calculated from Eq. (4). The experimental data for the second absorption peak were fitted by Eqs. (7), (8), and (9) using N, ε_s, ε_h, ω_p, t_j, and σ_{mj} as the variables. The values of r_j were taken from the histogram shown in Fig. 2. In Fig. 5 we show the experimental data and theoretically fitted curves for both the peaks in the cases of two specimens, viz., those subjected to oxidation treatments at 513 and 583 K, respectively. The experimental data are shown by the dotted curves, and the theoretical fits are given by the solid lines as indicated in the figure caption. To avoid congestion in the figure the results for other specimens have not been shown. It should be noted, however, that the agreement between theory and experiment in all cases is equally satisfactory. In these calculations we have taken $V_F = 1.4 \times 10^{15}$ nm/sec.[25]

In the above fitting six adjustable parameters have been used. Some doubts may be cast on the uniqueness of these numbers obtained after the theoretical fitting. However, the following discussion will show that these values are consistent with the physical situation in the present sample system. The values of $\varepsilon_h = 3.8$ and $\varepsilon_s = 11.0$ were obtained by least-squares fitting in the cases of all the six specimens. The ε_h value corresponds to dielectric permittivity of the host medium, which is essentially silica glass. The value of 3.8 is in agreement with the dielectric constant of silica glass.[27] The value of $\varepsilon_s = 11.0$ corresponds to the dielectric constant of Ag_2O as measured on a pure Ag_2O pellet by the authors.[28] In the present case, ε_s refers to the dielectric permittivity of the shell which comprises of Ag_2O. Thus the extracted values of ε_h and ε_s are in agreement with experimental values determined independently.

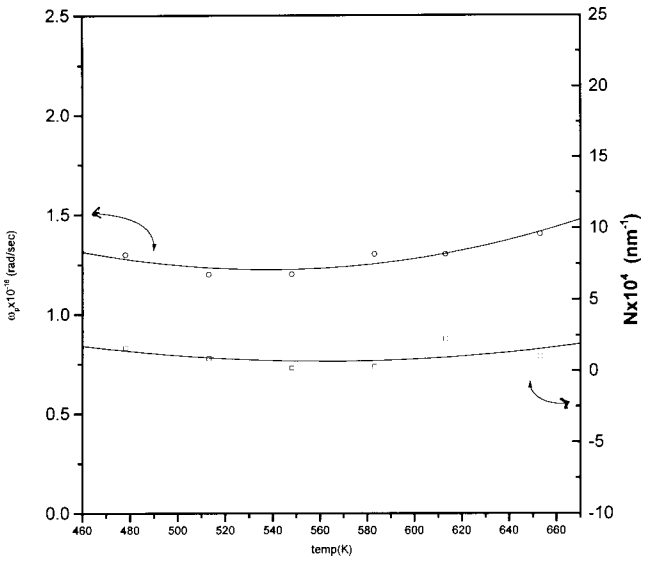

FIG. 6. Variation of N and ω_p (extracted by least-squares fitting) as a function of oxidation temperature: N (○) and ω_p (□).

The values of N—the number of particles with core-shell structure—as extracted by the theoretical fitting are plotted as a function of the oxidation temperature in Fig. 6. It is seen that the number shows a minimum at around 550 K. The points in this figure are the values determined by the fitting procedure, and the line has been drawn to guide the eye. This minimum is ascribed to the presence of two different processes competing with each other, viz., the Ostwald ripening,[29] which involves bigger metal particles gobbling up the smaller ones, and the oxidation of the metal particles. Above around 550 K the kinetics of the oxidation process becomes faster, and as a result, the value of N shows an increasing trend. Using the values of N as obtained for different specimens, we have estimated a volume fraction of the composite nanoparticles as ranging from 0.01 to 0.08. Such a low volume fraction justifies the estimation of polarizability by Eq. (7).

The extracted values of ω_p are also shown in Fig. 6 as a function of the oxidation temperature. The solid line is drawn to guide the eye. It is evident from these data that the ω_p values are smaller than that calculated (1.4×10^{16} rad/sec) on the basis of bulk silver electron density,[25] but are within 3% of the latter. There is a shallow minimum as a function of temperature. This is believed to arise due to the presence of silver particles exhibiting a metal-insulator transition in specimens subjected to oxidation treatments up to a temperature of 548 K. Above this temperature more and more particles show conductivity higher than Mott's minimum metallic conductivity (see below). Hence the ω_p values tend to

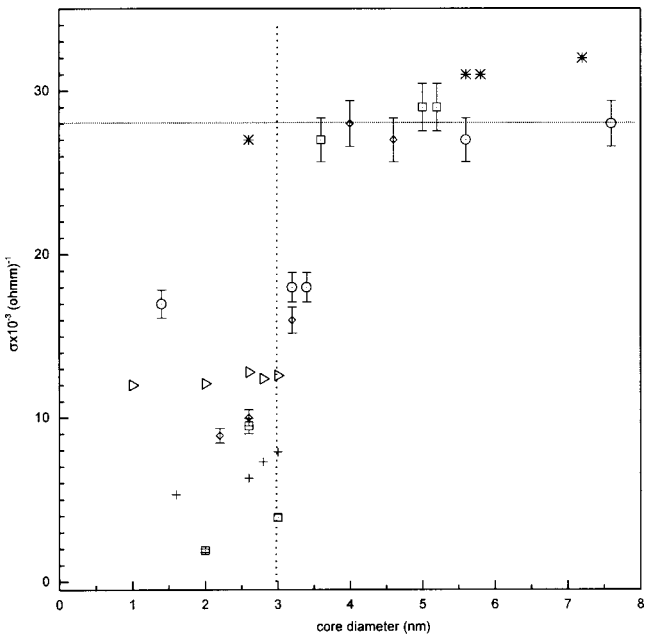

FIG. 7. Extracted conductivity (σ_{mj}) as a function of core diameter $2(r_j - t_j)$ for different specimens: (▷) specimen No. 1, (□) specimen No. 2, (+) specimen No. 3, (*) specimen No. 4, (◇) specimen No. 5, and (○) specimen No. 6.

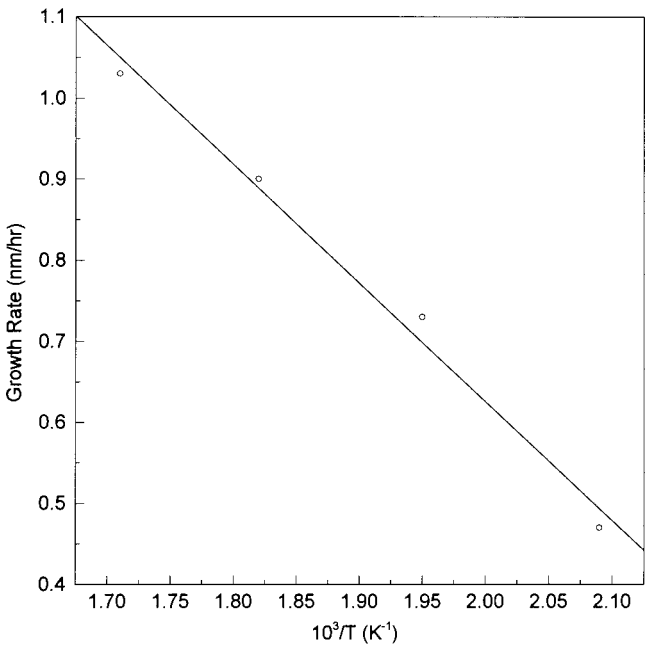

FIG. 8. Variation of shell growth rate (in nm/h) as a function of inverse temperature.

that calculated on the basis of bulk metallic silver. This is consistent with the fact that at higher oxidation temperatures some of the Ag_2O gets reconverted into metallic silver, thereby increasing the average diameter of metallic silver core within the composites.

We have summarized the extracted values of $2(r_j - t_j)$ denoting the silver-metal-core diameter and the corresponding values of σ_{mj} in Fig. 7 for the different specimens investigated. It is interesting to note that for core diameters equal to or less than 3 nm the electrical conductivity is less than $\sim 2.8 \times 10^4\ \Omega^{-1}\,\mathrm{m}^{-1}$. The latter is in reasonable agreement with Mott's minimum metallic conductivity as calculated in the case of silver. A few of the extracted parameters, however, do show this metal-insulator transition even for diameters greater than 3 nm. This is believed to be due to the discrete diameter values taken for our calculation. The discrete r_j values were taken from the histograms of particle sizes as exemplified by Fig. 2. If we now use this conclusion and extend the same to the results obtained from the first peak, as discussed earlier, we can come to the inference that the first peak arises due to the presence of silver particles of diameters less than ~3 nm, which were not affected by the oxidation treatment.

We have also considered the rate of growth of the oxide layer in our experiments. The oxide layer thicknesses as determined by least-squares fitting for different samples having diameters as shown in Fig. 2 were found to have values in the range 1.0–10.6 nm depending on the diameter of the metal particles and the oxidation treatment. Taking the thickness of the shell in different heat-treated specimens as extracted by the theoretical analysis described above corresponding to the median diameter for the temperature concerned, we have estimated the overall growth rate for the oxide nanoshell. We have taken the relevant data for specimens 1–4. The results for the other specimens are ignored because the process becomes complicated in those cases. Both oxidation and reduction mechanisms operate simultaneously in the latter. It is known that the kinetically controlled growth rate for an oxidation process is related to temperature by an equation of the type[30]

$$\dot{g}\,\alpha \exp(-\phi/kT), \tag{10}$$

where ϕ is the activation energy for diffusion of oxygen atoms in the nanocomposite concerned, k is the Boltzmann constant, and T is the temperature. Figure 8 gives a plot of growth rate (in nm/h) versus inverse temperature. From the slope of the straight line, which can be fitted to the calculated points, we have estimated a value of the activation energy as ~0.29 eV. This appears to be consistent with the activation energy of diffusion of oxygen atoms in a silicate glass.

In summary, we have prepared silver-silica nanocomposites by an electrodeposition technique. Silver oxide nanoshells on metallic silver particles have been grown by subjecting the nanocomposites to an oxidation treatment in the temperature range 478–653 K. Optical absorption spectra in the wavelength range 250–800 nm were recorded for films prepared by dispersing these nanocomposites in a polystyrene matrix. Two absorption peaks were observed: one around 370 nm and the other varying in the range 550–700 nm. The first one is ascribed to the plasmon resonance of silver nanoparticles, and the second one is shown to arise due to the presence of silver-core–silver-oxide shell nanostructure in the material. The experimental data have been analyzed by the relevant theory of scattering from ultrafine composite particles. This analysis shows that nanoshells of thicknesses in the range 1.0–10.6 nm are grown on the metal core depending on the oxidation temperature. The extracted

values of electrical conductivity indicate that particles having a metal core diameter of ~3 nm and less show a metal-insulator transition. The electrical conductivities for metallic particles responsible for the first absorption peak are less than Mott's minimum metallic conductivity. This implies that these particles have diameters less than 3 nm. Finally, the growth rate of the nanoshell when analyzed on the basis of a diffusion mechanism gives an activation energy of 0.29 eV, which is consistent with the activation energy for oxygen diffusion in a silicate glass.

ACKNOWLEDGMENTS

K.C. acknowledges CSIR, New Delhi, for support. D.C. thanks DST, New Delhi, for support of this research.

[1] J. W. Haus, H. S. Zhou, I. Honma, and H. Komiyama, J. Appl. Phys. **73**, 1043 (1993).
[2] A. Chatterjee and D. Chakravorty, Appl. Phys. Lett. **60**, 138 (1992).
[3] T. Fukumi, Rev. Laser Eng. **21**, 1151 (1993).
[4] H. S. Zhou, I. Honma, H. Komiyama, and J. W. Haus, Phys. Rev. B **50**, 12 052 (1994).
[5] Z. Gaoling, H. Kozuka, and S. Sakka, J. Sol-Gel Sci. Technol. **4**, 37 (1995).
[6] P. C. Ohara, D. V. Leff, J. R. Heath, and W. M. Gelbart, Phys. Rev. Lett. **75**, 3466 (1995).
[7] G. De, L. Tapfer, M. Catalano, G. Battaglin, F. Caccavale, F. Gonella, P. Mazzoldi, and R. F. Haglund, Jr., Appl. Phys. Lett. **68**, 3820 (1996).
[8] R. P. Andres, J. D. Bielefeld, J. I. Henderson, D. B. Janes, V. R. Kolagunta, C. P. Kubiak, W. J. Mahoney, and R. G. Osifchin, Science **273**, 1690 (1996).
[9] R. P. Andres, T. Bein, M. Dorogi, S. Feng, J. I. Henderson, C. P. Kubiak, W. Mahoney, R. G. Osifchin, and R. Reifenberger, Science **272**, 1323 (1996).
[10] R. D. Averitt, D. Sarkar, and N. J. Halas, Phys. Rev. Lett. **78**, 4217 (1997).
[11] G. Mie, Ann. Phys. (Leipzig) **25**, 377 (1908).
[12] C. G. Granqvist, N. Clander, and O. Hunderi, Solid State Commun. **31**, 249 (1979).
[13] D. Das and D. Chakravorty, Appl. Phys. Lett. **76**, 1273 (2000).
[14] D. Das, S. Roy, J. W. Chen, and D. Chakravorty J. Appl. Phys. (to be published).
[15] S. Bandyopadhyay and D. Chakravorty, J. Mater. Res. **12**, 2719 (1997).
[16] Sourish Banerjee, Soomit Banerjee, Anindya Datta, and Dipankar Chakravorty, Europhys. Lett. **46**, 346 (1999).
[17] B. Roy and D. Chakravorty, J. Phys.: Condens. Matter **2**, 9323 (1990).
[18] R. H. Doremus, J. Chem. Phys. **42**, 414 (1965).
[19] S. Banerjee, A. K. Maity, and D. Chakravorty, J. Appl. Phys. **87**, 8541 (2000).
[20] C. G. Granqvist and D. Hunderi, Phys. Rev. B **16**, 3513 (1977).
[21] R. C. West, *CRC Handbook of Chemistry and Physics*, 70th ed. (Chemical Rubber, Boca Raton, FL, 1989–1990), p. D-46.
[22] J. C. Maxwell-Garnet, Philos. Trans. R. Soc. London, Ser. A **203**, 385 (1904).
[23] A. Chatterjee and D. Chakravorty, J. Phys. D **22**, 1386 (1989).
[24] U. Kreibig, J. Phys. F: Met. Phys. **4**, 999 (1974).
[25] C. Kittel, *Introduction to Solid State Physics* (Wiley, New York, London, 1961), p. 374.
[26] N. F. Mott and E. A. Davis, *Electronic Processes in Non-Crystalline Materials* (Clarendon, Oxford, 1979), p. 26.
[27] *Handbook of Chemistry and Physics* (Chemical Rubber, Cleveland, OH, 1962), p. 2626.
[28] S. Banerjee and D. Chakravorty (unpublished).
[29] S. C. Jain and A. E. Hughes, J. Mater. Sci. **13**, 1611 (1978).
[30] R. W. Cahn, *Physical Metallurgy* (North-Holland, Amsterdam, 1965), Chap. 10.